1. Introduction

Rb-Sr and Sm-Nd isotope tracers are widely used in geochronology to study the formation and evolution of Earth and other planets. Thus, they are of great importance in isotope geochemistry research. In recent years, with the rapid development of novel multi-collector inductively coupled plasma mass spectrometer (MC-ICPMS) isotope analytical instruments, research based on traditional and non-traditional stable isotopes, such as Li, Be, Mg, Si, Fe, Cu, Zn, and Mo, has driven the study of isotope geochemistry in areas such as environmental science, climate, and mineral deposits (Salters, 1994; Halliday et al., 1995; Blichert-Toft et al., 1997; Blichert-Toft, 2001; Műnker et al., 2001; Kleinhanns et al., 2002; Beard et al., 2003; Teng et al., 2009; Dong and Wasylenki, 2016; Gao et al., 2016; Ryu et al., 2016; Zhu et al., 2016; Zheng et al., 2017). Currently, with the rapid development of modern analytical instruments, the bottleneck in isotope geochemistry research has shifted from instrumental analysis to sample processing. The speed of instrumental analysis has been reduced from ~40 min per sample using the traditional thermal ionization mass spectrometer (TIMS) to a few minutes using MC-ICPMS; this is a significant increase in efficiency. However, the separation speed of isotopes in geological samples has not improved much. Scientists have attempted to simultaneously separate multiple isotopes in one sample dissolution using different approaches. These include dissolving the sample using a combination of solution and melting methods, designing new separation methods, and changing the separation process. They were able to rapidly separate multiple isotopes such as Sr-Mg, Lu-Hf, Rb-Sr, and Sm-Nd in one sample dissolution (Bizzarro et al., 2003; Ulfbeck et al., 2003; Lapen et al., 2004; Yang et al., 2010; Bast et al., 2015; Sikdar and Rai, 2017), moderately improving the separation ability. Other high-speed analytical instruments, such as ion-exchange chromatography, could also rapidly separate Ca and Mg ions, achieving ten times the efficiency previously reported (Blättler and Higgins, 2014); this was a great improvement. The adoption of automated separation systems using HPLC or prepFAST-MC (ESI, USA) systems has also made the unmanned automated

separation of isotopes possible (Meynadier et al., 2006; Field et al., 2012; Romaniello et al., 2015; Enge et al., 2016).

In this work, the aim was to make the conventional ion exchange column to speed up the separation process without changing the current experimental conditions nor purchasing special equipment. Thus, we attempted to use high-purity N_2 in our present system to accelerate the flow of the mobile phase in the ion exchange column. We predicted that this would enhance the adsorption-desorption efficiency of ions between the mobile and stationary phases and afford a more efficient separation of Sr, and Nd isotopes than that achieved in ordinary lab conditions.

2. Materials and Methods

2.1. Chemicals and materials

Water used in the experiments (18.2 $M\Omega \cdot cm^{-1}$) was purified by Milli-Q (Elix-Millipore, Merck, Darmstadt, Germany). HNO_3, HCl, and $HClO_4$ distilled on a quartz sub-boiling distillation device. HF was prepared using a PFA DST-1000 sub-boiling acid distillation unit (Savillex, Eden Prairie, Minnesota, USA).

AGV-2, the international standard sample for the whole-rock powder of andesite, was purchased from the United States Geological Survey (USGS). BCR-2, the international standard samples for the whole-rock powder of basalt, were purchased from the USGS. Two pure copper samples NWU-Cu-A (Alfa Aesar, Stock #43822, Lot #E23T019) and NWU-Cu-B (Alfa Aesar, Stock #10974, Lot #I28Q011) (Yuan et al., 2017) were purchased from Alfa Aesar, Johnson Matthey Co. and used to prepare Cu standard solutions.

Cation-exchange resin AG50W-X8 (200-400 mesh, batch 142-1451) and AGMP-1M (200-400 mesh, batch 141-1851) were purchased from Bio-Rad (Richmond, CA, USA); pre-packed extraction chromatography material (Ln Spec, 100–150 μm particle size, 2 mL, Batch FLNA140429) and Sr Spec resin (100–150 μm particle size, 2 mL, Batch FSRA141030) were purchased from Eichrom Industries (Darien IL, USA).

Chalcopyrite samples (No. TC-15 and TC-17) were collected from the Dexing copper mine in Jiangxi province. The samples did not contain any inclusions; they were crushed and picked with binoculars, leached in 50% HNO_3, and subsequently ultrasonicated three times to remove cracks and surface contaminants. The purified samples were dried and ground by hand using an agate mortar to #200 mesh.

2.2. Instruments

Isotopic compositions of Cu, Sr, and Nd were measured at the State Key Laboratory of Continental Dynamics, Northwest University, on a Nu Plasma II MC-ICPMS (Nu Instruments, Wrexham, UK) with the Faraday cup in static mode. The sample separation curves were measured by the wet method using a Varian 820-MS quadrupole ICP-MS (Jena, Germany) under conventional sensitivity. The instrument parameters are listed in Table 1. Samples were injected using a 100 μL/min glass concentric atomizer by self-absorption, with 2% HNO_3 as the sample solvent. The Cu isotope ratio was corrected using the SSB method (NUW-Cu-A as the standard) (Yuan et al., 2017); Sr isotope measurements were performed on an NIST SRM 987. Mass fractionation was corrected with $^{86}Sr/^{88}Sr = 0.1194$. During measurements, the value for NIST SRM 987 was determined as 0.710254 ± 25 (2 SD, n = 20); this is consistent with the reference value of 0.710250 ± 30 (2 SD) within the range of error (the reference value was quoted from GeoReM database as the average value of ID-TIMS published results after the year 2000) (Jochum et al., 2005). Nd isotope correction was performed using $^{146}Nd/^{144}Nd = 0.7219$ by the exponential law method, with JNDi-1 as the standard solution. The measured value was determined as 0.512107 ± 20 (2 SD, n = 20); this agrees with the reference value of 0.512115 ± 7 (Tanaka et al., 2000) in the range of 2 SD.

The samples were dissolved in a high-temperature and high-pressure (HTHP) dissolution bomb, and the clear solution was centrifuged at 13,000 rpm for 10 min (Eppendorf 5415D, Germany) to remove any insoluble sediment before loading into the column.

Table 1. Instrumental parameters of multiple-collector inductively coupled plasma mass spectrometry (MC-ICPMS) and quadruple ICPMS.

ICPMS model	Nu Plasma II	Varian 820MS
Plasma gas flow rate, L/min	13.0	17
Auxiliary gas flow rate, L/min	0.8	1.7
Makeup gas, L/min	0.6	0.22
RF Power, W	1300	1400
Accelerating voltage, V	6000	-
Sample uptake rate, μL/min	100	200
Sensitivity	Cu: 22V/ppm	In: 1 Mcps / ppb

2.3. Cu isotope separation

The Cu isotope separation process was established using naturally occurring chalcopyrite samples (TC15). The samples were dissolved in a concentrated HF/HNO_3 mixture (v/v = 1:1) in a HTHP dissolution bomb at 190 ºC for 24 h until they became clear. They were subsequently dissolved in HCl to form 8 mol/Lsolutions.

The Cu isotopes were separated using AGMP-1M resin. Prior to its first use, the resin was soaked in high-purity water for 24 h. The supernatant was decanted and the column was packed using the wet packing method. Next, 0.5 mol/L HNO_3 and 8 mol/L HCl (+ 0.001% H_2O_2; volume fraction) and MQ water were used to elute the column alternatively; 8 mol/L HCl (+ 0.001% H_2O_2; volume fraction) were used to precondition the resin. The volume of the resin was adjusted to 2 mL. After the sample was loaded, matrix elements (Na, Mg, Al, Ca, Ti, Cr, Ni, and Mn) were removed with 8 mL of 8 mol/L HCl (+ 0.001% H_2O_2). Next, 22 mL of the same solvents were used to elute and collect Cu while 18 mL of 2 mol/L HCl was used to collect Fe. The elution process is listed in Table 2.

Table 2. Column chromatography procedure for 2mL AGMP-1M Bio-Rad resin

Step	Solvent	Volume (mL)	Note
1	8 M HCl + 0.001% H_2O_2	6 + 6	
2	Milli-Q H_2O	6	Preparation
3	0.5 M HNO_3	6 + 6	

4	Milli-Q H_2O	6	
5	8 M HCl + 0.001% H_2O_2	2 + 6	Preconditioning
6	8 M HCl + 0.001% H_2O_2	0.05	Loading sample
7	8 M HCl + 0.001% H_2O_2	2 + 6	Eluting matrix
8	8 M HCl + 0.001% H_2O_2	22	Collecting Cu
9	2 M HCl	20	Collecting Fe

This Cu isotope separation method achieved the separation of Cu and Fe from other matrix elements with a recovery rate of >99.9%. However, the process lasted for 12 h and was time-consuming. Therefore, our aim in this study was to improve the elution speed by applying pressure to the normal ion-exchange column, thereby reducing the separation time.

2.4. Sr-Nd isotope purification

A study on the separation process and pressurized separation scheme for Sr-Nd isotopes was performed with the USGS standard andesite sample AGV-2 as an example. The powdered standard sample was sealed and dissolved in a HTHP dissolution bomb and transferred into a 1.7 mol/L solution in HCl. Sr-Nd isotopes were separated in two steps (Table 3), the first to separate Sr and REEs and the second to separate Nd and other rare earth elements. For samples with a high Rb/Sr ratio (some granites), an additional purification step was performed on Sr after the first separation, using Sr spec resin (Table 3), so that the eluent collected at the end of the experiment presented a Rb/Sr ratio <0.0005. These three steps lasted for 5 h, 7 h, and 6 h, respectively. The whole process which lasts 2 days to complete Sr and Nd isotope separation, including solvent dry-down is rather time-consuming.

2.5. Design of the pressurization column

First, a screw thread was crafted onto the top of the existing ion exchange column. A polytetrafluoroethylene cap with a gas connector at the top was then created to

assemble a pressurized exchange column (Figure 1). The resin part (φ = 6 mm × 80 mm) could hold 2 mL of resin while 18 mL of solution could be added to the space above the resin (φ = 28 mm × 30 mm) each time. High-purity N_2 gas was delivered via PU tubing (4 mm i.d.). The gas flow was precisely controlled with an MFC (flow rate range = 0–100 mL/min).

Table 3. Chemical separation scheme for Sr and rare earth element (REE) isotopes with AG50W-X8 resin (resin volume 2 mL)

Step	Solvent	Volume (mL)	Note
First step: purify Sr and REE			
1	6 M HCl	1 + 2 + 6	Preparation
2	1.7 M HCl	1 + 3 + 8	Preconditioning
3	1.7 M HCl	1	Loading sample
4	1.7 M HCl	0.5 + 1 + 10	Eluting matrix
5	3 M HCl	6	Collecting Sr
6	6 M HCl	10	Collecting REEs
Second step: purify Nd using Ln-Spec resin			
1	Citric acid	10	Preparation
2	6 M HCl	2 + 8	
3	MQ H_2O	2 + 8	
4	0.25 M HCl	2 + 4	Preconditioning
5	0.25 M HCl	0.25	Loading sample
6	0.25 M HCl	1 + 1 + 2	Eluting matrix
7	0.25 M HCl	10	Collecting Nd
Third step: purify Sr using Sr-spec resin for high Rb/Sr samples			
1	Citric acid	10	Preparation
2	8 M HNO_3	2 + 8	Preconditioning
3	8 M HNO_3	0.5	Loading sample
4	8 M HNO_3	1 + 1 + 18	Eluting matrix
5	0.05 M HNO_3	10	Collecting Sr

Figure 1.

3. Results and Discussions

3.1. Effects of rapid pressurized separation on the separation curve and recovery rate

Rapid sample separation, via the installation of a simple pressurization device to our current setup, was achieved in two ways. One option was to apply pressure to the whole separation process; this included every step from the first eluting step to the final sample collection step (full-pressure mode). The second option was to apply pressure only during sample elution while keeping a normal flow rate from sample loading to collection; this method still made use of the existing isotope separation scheme (partial-pressure mode). We first investigated the effects of pressurized rapid separation (ion exchange resin column) on the separation curve of light and heavy isotopes. We evaluated the reliability and feasibility of this method by comparing the separation curves and recovery rates, as well as isotope ratios of Cu isolated and purified by AGMP-1 resin, under different pressure conditions.

Table 4. The time required for 10 mL of solution (6 M HCl) to pass through the AGMP-1 ion exchange column at different N_2 flow rates and the separation time for the whole process

Gas flow rate, mL/min	**0**	**20**	**40**	**60**	**80**	**100**
Duration time of 10 mL solvent (min)	56.5	2	1.8	1.7	1.4	1.4
Total separation time (h)	12	4.5	4	3.5	3	3

The gas flow rates were 0, 20, 40, 60, 80, and 100 mL/min. Improvements on the separation speed by different gas flow rates are listed in Table 4. The eluent flow rate

was slightly different for the four resins. Without gas pressure, AG50W-X8, Ln Spec resin, Sr Spec resin, and AGMP-1 resin exhibited average eluent velocities of 8.5, 12, 12, and 10.7 mL/h, respectively. For AGMP-1, under different gas flow rates, the solvent flow rate increased with increasing gas flow rate. When 20, 40, 60, 80, and 100 mL/min gas flows were introduced, the elution time for 10 mL of solution decreased from 56 min at no gas flow to a range of 2–1.4 min (Table 4). The Cu separation curves displayed slight variations under different gas flow rates (Figure 2). The highest peaks all appeared at approximately the same time that the gas flow rate was increased, however, the separation peaks broadened (Figure 2), especially when 80 and 100 mL/min gas flows were applied. The signals for matrix elements (Na, Mg, Ca, and K) also exhibited the same trend of broadening; moreover, slight lagging of tailing peaks was observed for matrix elements starting at a flow rate of 40 mL/min. The exchange time in the column was <2 min for gas flow rates ≤20 mL/min and tailing for matrix element peaks and Cu and Fe separation peaks started at 40 mL/min. The reason for the peak shift is probably caused by the ion exchange efficiency changing at high fluid flow rate. Thus, we decided to use 20 mL/min gas flow as the standard acceleration. Under these conditions, the separation time for the whole process was reduced from the initial 12 h to 4.5 h, an approximately three-fold increase in efficiency. We considered this as a significant improvement.

Figure 2.

Non-traditional stable isotopes are prone to fractionation in the ion exchange process. The whole process (separation and purification) therefore requires a recovery rate >99.5%. We measured the recovery rate of Cu under different gas flow conditions. The results established that using the conventional separation curves with no added gas flow, a recovery rate >99.9% was afforded for a gas flow rate ranging from 0 to 60 mL/min. At flow rates of 80 and 100 mL/min, the Cu peak broadened

and the recovery rate decreased to 99.3% and 99.2%, respectively. When the gas flow rate was 20 mL/min, the separation curve was not affected and a 99.95% recovery rate was achieved. Based on the separation of Cu, the recovery of Fe isotopes was also determined after the Cu fractions were collected. This displayed a gas flow rate relationship similar to that observed in Cu. At a gas flow rate of 60 mL/min, the recovery of Fe was slightly less than that of Cu while at 20 mL/min, both presented recovery rates >99.9% (Table 5).

Table 5. Recovery of Cu and Fe isotopes under different N_2 gas flow rate

Gas flow (mL/min)	0	20	40	60	80	100
Cu recovery (%)	99.99	99.95	99.95	99.97	99.34	99.15
Fe recovery (%)	99.99	99.92	99.93	99.61	98.18	98.12

3.2. Effects of rapid separation on analysis accuracy

3.2.1. Analytical results for Cu isotopes

The standard NWU-Cu-A and natural sulfide (TC15 and TC17) samples were passed through the exchange column using no-pressure mode, partial-pressure mode (20 mL/min), and full-pressure mode (20 mL/min), respectively. The recovery rates of all three methods were >99.9%, and δ^{65}Cu was determined as 1.00 ± 0.02 ‰ (2s, n = 4), 0.90±0.05 ‰ (2s, n = 5), and 0.93 ± 0.03 ‰ (2s, n = 4) (Table 6). These results are consistent with the reference value within the 2s error range(Yuan et al., 2017). The Cu isotope compositions of the chalcopyrite TC-15 and TC-17 samples, purified with the three modes, agreed well with each other within the 2s error range. The separation efficiency was, however, greatly improved with the separation time for "partial-pressure" and "full-pressure" modes reduced from the initial 12 h to 5 h and 4 h, respectively; a 2.4- and three-fold increase in efficiency, respectively.

Table 6. Determination of δ^{65}Cu for NWU-Cu-A and sulfides by the standard-sample bracketing (SSB) method under different pressure separation modes

Gas Mode	**No-pressure***	**Full-pressure**	**Partial-pressure**	**Ref**

NWU-Cu-A	1.00 ± 0.02	0.90 ± 0.05	0.93 ± 0.03	0.96 ± 0.03
TC-15	-0.78 ± 0.02	-0.76 ± 0.02	-0.77 ± 0.03	
TC-17	-0.77 ± 0.02	-0.80 ± 0.02	-0.78 ± 0.02	

*"No-pressure" signifies that no N_2 was applied for pressurized separation during any part of the process. "Full-pressure" signifies that N_2 was introduced for pressurized separation in all steps of the process. "Partial-pressure" signifies that pressure was applied during washing and preconditioning of the ion-exchange column but not from sample loading to the collection of target isotopes; n=4; NWU-Cu-B was analyzed as standard; in ‰. Ref value was taken from Yuan et al., Geostandards and Geoanalytical Research, 2017, 41(1):77-84(Yuan et al., 2017).

3.2.1. Sr, Nd isotopes analysis

Sr and Nd isotopes are widely used in the study of isotope geochemistry, such as in isotope tracing and Sm-Nd and Rb-Sr dating. However, the separation of these two isotopes is time-consuming, especially for Nd. This generally requires the simultaneous separation of rare earth elements during the separation of Sr and its subsequent purification from REE. One sample analysis therefore often takes 2–3 d to complete. The Sr-Nd isotope separation was accelerated by the proposed pressurization method. The analytical results for AGV-2 using the "no-pressure" mode, the "partial-pressure" mode (20 mL/min), and the "full-pressure" mode (20 mL/min) are listed in Table 7. The results indicate that the Nd and Sm isotopes in the rock sample were well separated by all three methods. The $^{144}Sm/^{144}Nd$ratios in the solutions were all $<10^{-5}$ and the Nd isotope compositions determined by all three methods were will in agreement with the reference within a 2s error range.

Table 7. Comparison of isotope separation of Sr and Nd in AGV-2, BCR-2, and BIR-1 under different pressure separation modes

Gas mode	$^{143}Nd/^{144}Nd$(±2s)	$^{87}Sr/^{86}Sr$(±2s)	References
AGV-2			
No-Pressure	0.512786(8)	0.703994(12)	
Full-Pressure	0.512781(8)	0.703986(14)	
Partial-Pressure	0.512783(6)	0.703994(8)	
Reference*	0.512786(28)	0.703992(66)	[Jochum et al., 2016]
	0.512781(13)	0.703978(19)	[Yang et al., 2010]
	0.512788	0.703979	[Li et al., 2015]
BCR-2			

No-Pressure	0.512638(10)	0.705020(20)	
Full-Pressure	0.512634(26)	0.705017(30)	
Partial-Pressure	0.512640(06)	0.705018(18)	
Reference*	0.512635(58)	0.70492(110)	[Jochum et al., 2016]
	0.512640(08)	0.705023(01)	[Yang et al., 2010]
	0.512635(12)	0.705015(14)	[Li et al., 2015]

* Reference values were cited from GeoReM preferred values (Jochum et al., 2016), MC-ICPMS(Yang et al., 2010) and TIMS (Li et al., 2015) measurements. All errors referred to 2SD. "No-Pressure" signifies that no N_2 was applied for pressurized separation during any part of the process. "Full-Pressure" signifies that N_2 was introduced for pressurized separation in all steps of the process. "Partial-Pressure" signifies that pressure was applied during washing and preconditioning of the ion-exchange column but not from sample loading to the collection of target isotopes. The no-pressure mode was repeated for 20 times while both the Full-Pressure and Partial-Pressure modes were run for 5 times.

To ensure the reproducibility and general applicability of the experimental scheme, we purified the Sr isotopes with a two-step separation and purification process. The separation of AGV-2 and BCR-2 by all three methods indicated the effective separation of Rb and Sr by both "partial-pressure" and "full-pressure" methods. The $^{85}Rb/^{88}Sr$ ratios were all $<1.8\times10^{-4}$ and the Sr isotope composition afforded was consistent with the reference within a 2s error range. These results confirmed the effective isolation and purification of Sr and Nd isotopes in geological samples by all three methods.

However, the efficiency of the different separation methods varied. In the traditional method with no N_2 and no pressurization, the two-step separation of Sr isotopes required 5 h and 6 h, respectively. Nd separation was performed in two steps, namely, the separation of REE followed by that of Sr; these lasted 7 h and 6 h, respectively. The conversion of the medium and drying-down of the sample required 4 h and 7 h for Sr and Nd, respectively. Overall, the whole process lasted for a total of 15 h and 20 h, respectively and usually had to be completed over two days. After the adoption of the "full-pressure" method, the two separation steps for Sr both were completed after 2 h so that with solvent conversion and drying, the whole process lasted a total of 8 h. Pressurization also reduced the two isolation and purification steps for Nd to 2.5 h and 2 h, respectively; thus, including solvent conversion, a total of 11.5 h was

required. Moreover, if some overlap time can be utilized, such as starting resin elution for the subsequent separation as the collected Sr and REE eluent is being dried, the separation time can be further reduced to <10 h. The "Partial-Pressure" method would take an additional 1-2 h when compared to the "full-pressure" gas mode.

4. Conclusion

In this study we succeeded in increasing the isotope separation and purification efficiency of the current ion exchange resin by introducing pressure with high-purity N_2. The results of the stable isotopes of Cu and the conventional isotopes of Sr and Nd demonstrated that under a N_2 flow rate of 20 mL/min, the recovery rate of Cu was >99.9% in both "full-pressure" mode and "partial-pressure" mode. The determined Cu isotope ratios were consistent with the references within a 2 SD error range. Furthermore, the time required was reduced from 10 h in the conventional method to 4 h in the proposed method. Sr and Nd isotope separation for whole-rock samples was shortened from the conventional 2 d to <10 h, a significant improvement in separation efficiency. The afforded isotope ratio agreed with the reference within the 2s error range. Our study provides a new approach for rapid isotope separation.

ACKNOWLEDGEMNETS

This work was co-supported by the National Science Foundation of China (Grants 41427804, 41421002, 41373004), Program for Changjiang Scholars and Innovative Research Team in University (IRT1281), and the MOST Research Foundation from the State Key Laboratory of Continental Dynamics.

References

Bast, R., Scherer, E. E., Sprung, P., et al., 2015. A rapid and efficient ion-exchange chromatography for Lu-Hf, Sm-Nd, and Rb-Sr geochronology and the routine isotope analysis of sub-ng amounts of Hf by MC-ICP-MS. *Journal of Analytical Atomic Spectrometry*, 30(11): 2323–2333

Beard, B. L., Johnson, C. M., Skulan, J. L., et al., 2003. Application of Fe isotopes to tracing the geochemical and biological cycling of Fe. *Chemical Geology*, 195(1–4): 87–117

Bizzarro, M., Baker, J. ,Ulfbeck, D., 2003. A new digestion and chemical separation technique for rapid and highly reproducible determination of Lu/Hf and Hf isotope ratios in geological materials by MC-ICP-MS. *Geostandards and Geoanalytical Research*, 27: 133–145

Blättler, C. L. ,Higgins, J. A., 2014. Calcium isotopes in evaporites record variations in Phanerozoic seawater SO₄ and Ca. *Geology*, 42(8): 711–714

Blichert-Toft, J., Chauvel, C. ,Albarède, F., 1997. Separation of Hf and Lu for high-precision isotope analysis of rock samples by magnetic sector-multiple collector ICP-MS. *Contrib Mineral Petrol*, 127: 248–260

Blichert-Toft, J., 2001. On the Lu-Hf isotope geochemistry of silicate rocks. *Geostandards and Geoanalytical Research*, 25: 41–56

Dong, S. ,Wasylenki, L. E., 2016. Zinc isotope fractionation during adsorption to calcite at high and low ionic strength. *Chemical Geology*, 447: 70–78

Enge, T. G., Field, M. P., Jolley, D. F., et al., 2016. An automated chromatography procedure optimized for analysis of stable Cu isotopes from biological materials. *Journal of Analytical Atomic Spectrometry*, 31(10): 2023–2030

Field, M. P., Romaniello, S. J., Gordon, G. W., et al., 2012. Automated sample preparation for radiogenic and non-traditional metal isotope analysis by MC-ICP-MS. *American Geophysical Union, Fall Meeting 2012, abstract #V23B-2823*

Gao, T., Ke, S., Teng, F.-Z., et al., 2016. Magnesium isotope fractionation during dolostone weathering. *Chemical Geology*, 445: 14–23

Halliday, A. N., Lee, D.-C., Christensen, J. N., et al., 1995. Recent developments in inductively coupled plasma magnetic sector multiple collector mass spectrometry. *International Journal of Mass Spectrometry, Ion Proc.*, 146/147: 21–33

Jochum, K. P., Nohl, U., Herwig, K., et al., 2005. GeoReM: A new geochemical database for reference materials and isotopic standards. *Geostandards and Geoanalytical Research*, 29(3): 333–338

Jochum, K. P., Weis, U., Schwager, B., et al., 2016. Reference Values Following ISO Guidelines for Frequently Requested Rock Reference Materials. *Geostandards and Geoanalytical Research*, 40(3): 333–350

Kleinhanns, I. C., Kreissig, K., Kamber, B. S., et al., 2002. Combined chemical separation of Lu, Hf, Sm, Nd, and REEs from a single rock digest: precise and accurate isotope determinations of Lu-Hf and Sm-Nd using multicollector-ICPMS. *Anal. Chem.*, 74: 67–73

Lapen, T. J., Mahlen, N. J., Johnson, C. M., et al., 2004. High precision Lu and Hf isotope analyses of both spiked and unspiked samples: A new approach. *Geochem. Geophys. Geosyst.*, 5: 01010, doi:01010.01029/02003GC000582

Li, C.-F., Chu, Z.-Y., Guo, J.-H., et al., 2015. A rapid single column separation scheme for high-precision Sr-Nd-Pb isotopic analysis in geological samples

using thermal ionization mass spectrometry. *Analytical Methods*, 7(11): 4793–4802

Meynadier, L., Gorge, C., Birck, J.-L., et al., 2006. Automated separation of Sr from natural water samples or carbonate rocks by high performance ion chromatography. *Chemical Geology*, 227(1–2): 26–36

Műnker, C., Weyer, S., Scherer, E., et al., 2001. Separation of high field strength elements (Nb, Ta, Zr, Hf) and Lu from rock samples for MC-ICP-MS measurements. *Geochem. Geophys. Geosyst.*, 2: Paper number 2001GC000183

Romaniello, S. J., Field, M. P., Smith, H. B., et al., 2015. Fully automated chromatographic purification of Sr and Ca for isotopic analysis. *Journal of Analytical Atomic Spectrometry*, 30(9): 1906–1912

Ryu, J.-S., Vigier, N., Decarreau, A., et al., 2016. Experimental investigation of Mg isotope fractionation during mineral dissolution and clay formation. *Chemical Geology*, 445: 135–145

Salters, V. J. M., 1994. 176Hf/177Hf determination in small samples by a high-temperature SIMS technique. *Anal. Chem.*, 66: 4186–4189

Sikdar, J. ,Rai, V. K., 2017. Simultaneous chromatographic purification of Si and Mg for isotopic analyses using MC-ICPMS. *Journal of Analytical Atomic Spectrometry*: DOI:10.1039/C1036JA00426A

Tanaka, T., Togashi, S., Kamioka, H., et al., 2000. JNdi-1: a neodymium isotopic reference in consistency with LaJolla neodymium. *Chemical Geology*, 168(3): 279–281

Teng, F.-Z., Rudnick, R. L., McDonough, W. F., et al., 2009. Lithium isotopic systematics of A-type granites and their mafic enclaves: Further constraints on the Li isotopic composition of the continental crust. *Chemical Geology*, 262(3-4): 415–424

Ulfbeck, D., Baker, J., Waight, T., et al., 2003. Rapid sample digestion by fusion and chemical separation of Hf for isotope analysis by MC-ICPMS. . *Talanta*, 59: 365–373

Yang, Y.-h., Zhang, H.-f., Chu, Z.-y., et al., 2010. Combined chemical separation of Lu, Hf, Rb, Sr, Sm and Nd from a single rock digest and precise and accurate isotope determinations of Lu–Hf, Rb–Sr and Sm–Nd isotope systems using Multi-Collector ICP-MS and TIMS. *International Journal of Mass Spectrometry*, 290(2–3): 120–126

Yuan, H., Yuan, W., Bao, Z., et al., 2017. Development of two New Copper Isotope Standard Solutions and their Copper Isotopic Compositions. *Geostandards and Geoanalytical Research*, 41(1): 77–84

Zheng, X.-Y., Beard, B. L., Lee, S., et al., 2017. Contrasting particle size distributions and Fe isotope fractionations during nanosecond and femtosecond laser ablation of Fe minerals: Implications for LA-MC-ICP-MS analysis of stable isotopes. *Chemical Geology*, 450: 235–247

Zhu, C., Liu, Z., Zhang, Y., et al., 2016. Measuring silicate mineral dissolution rates using Si isotope doping. *Chemical Geology*, 445: 146–163

Figure Captions:

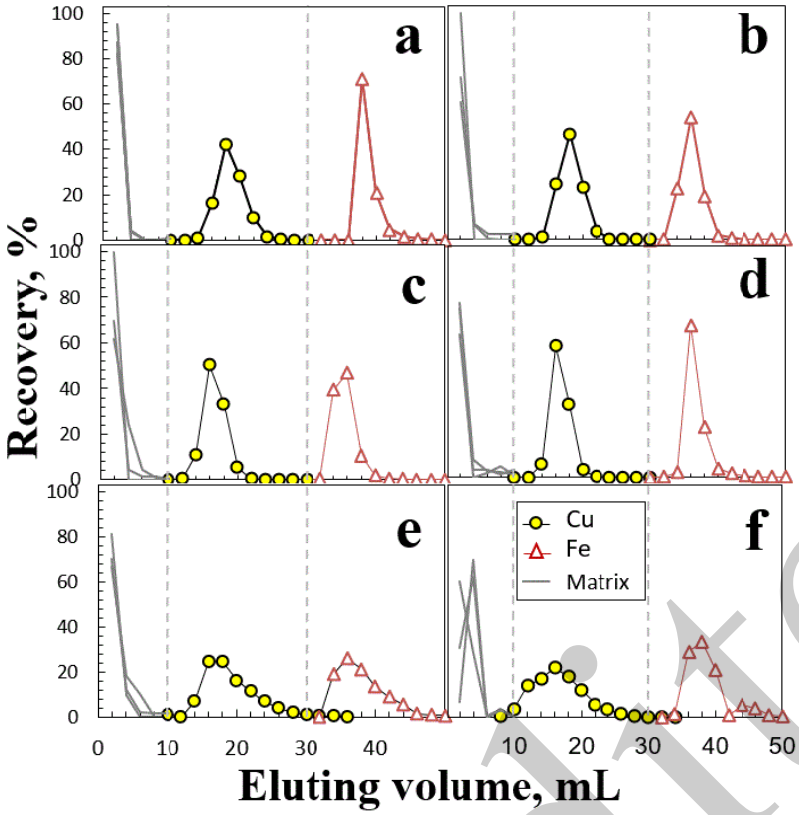

Fig. 1. Design of the pressurized ion-exchange resin column. (a) The design of a single pressurized column; (b) a schematic diagram for the simultaneous batch processing of 10 columns. High-purity N_2 was introduced in a controlled manner with mass flow controller (MFC).

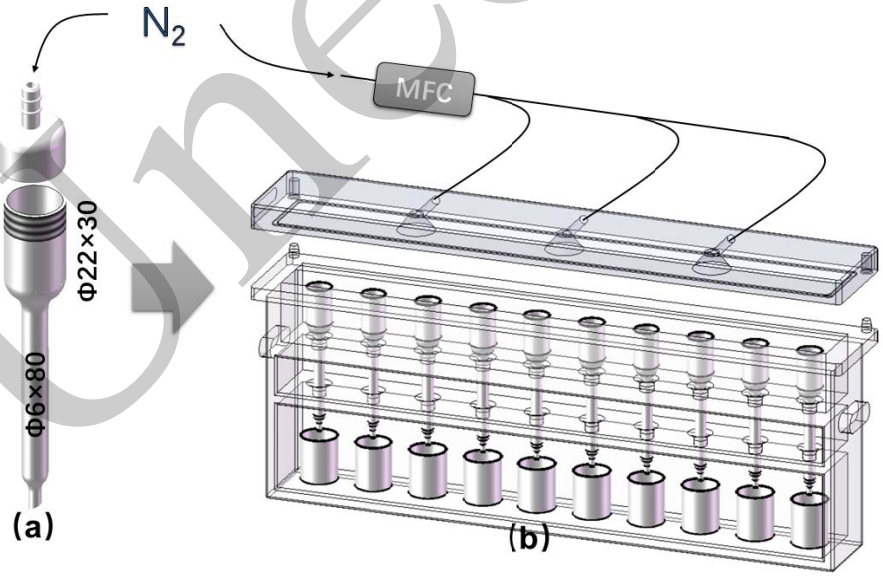

Fig. 2. Comparison of separation curves of Cu isotopes in chalcopyrite at different gas flow rates (0–100 mL/min) using an AGMP-1 resin column. (a) 0 mL/min; (b) 20 mL/min; (c) 40 mL/min; (d) 60 mL/min; (e) 80 mL/min; (f) 100 mL/min.